Supplemental Figures

Figure S1

A

B

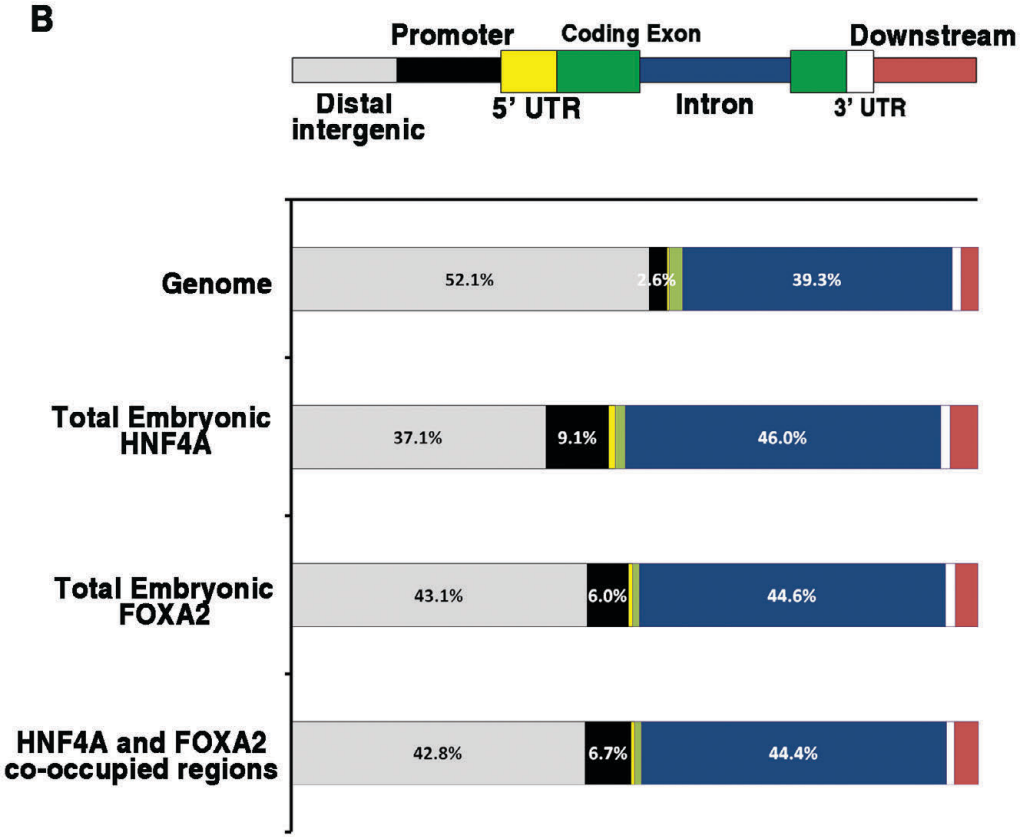

Figure S2

A

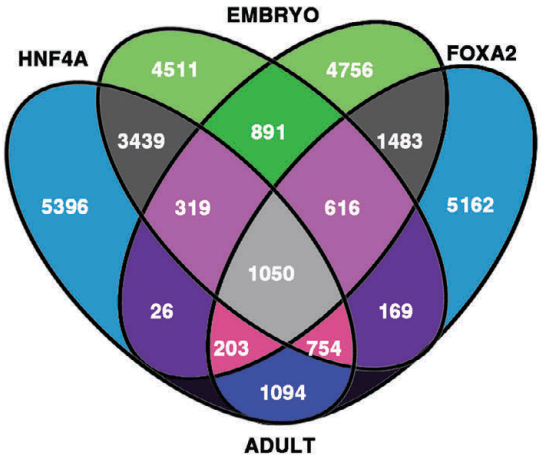

B

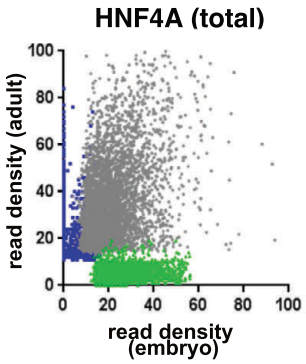

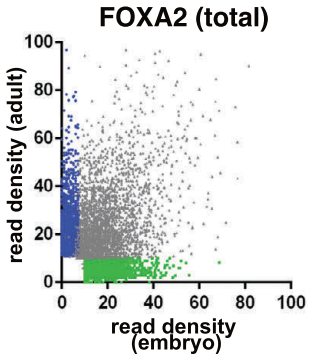

C

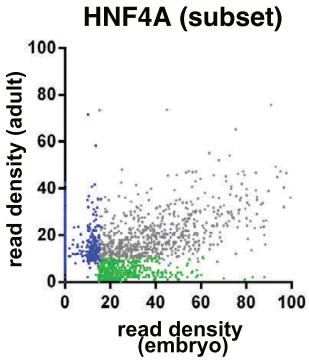

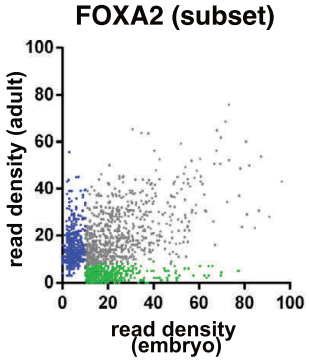

Figure S3

A

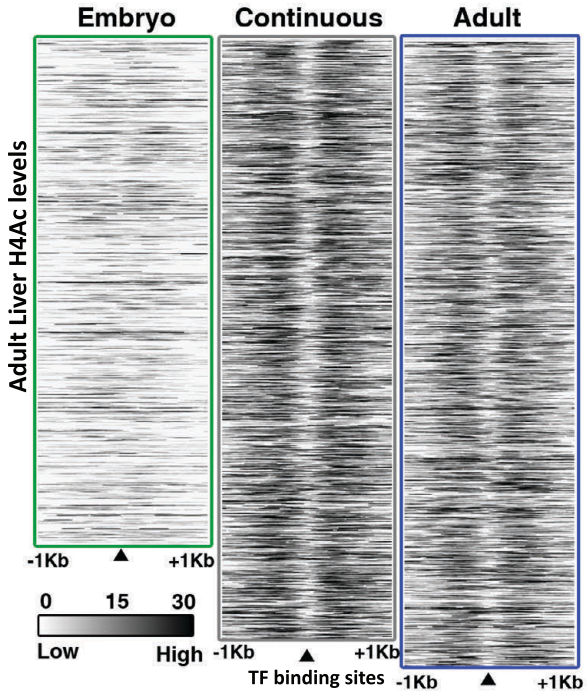
Embryo
Continuous
Adult
Adult Liver H4Ac levels
-1Kb
+1Kb
0
15
30
Low
High
TF binding sites

B

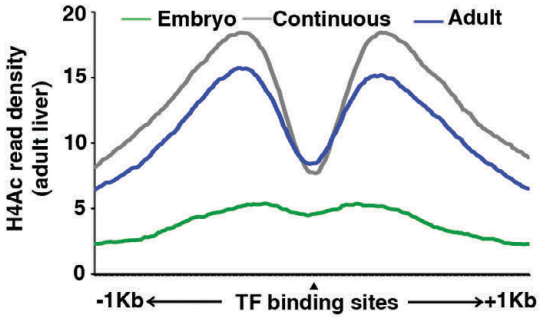
Embryo
Continuous
Adult
H4Ac read density (adult liver)
20
15
10
5
0
-1Kb
TF binding sites
+1Kb

Figure S4

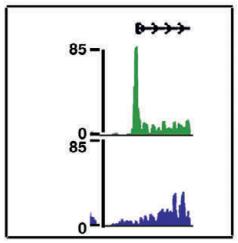

A

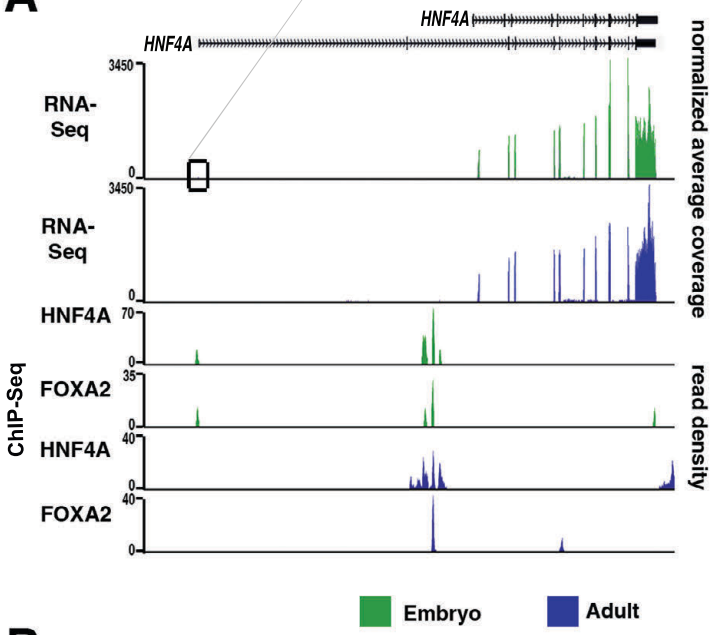

B

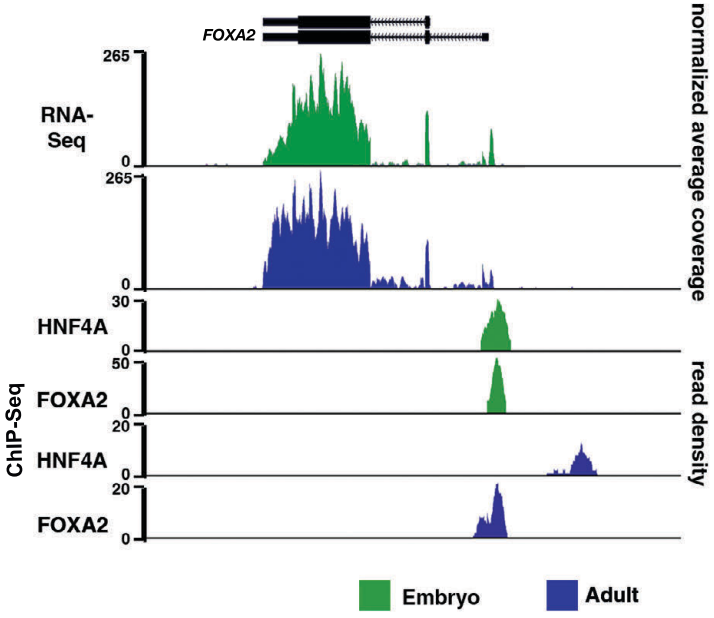

C

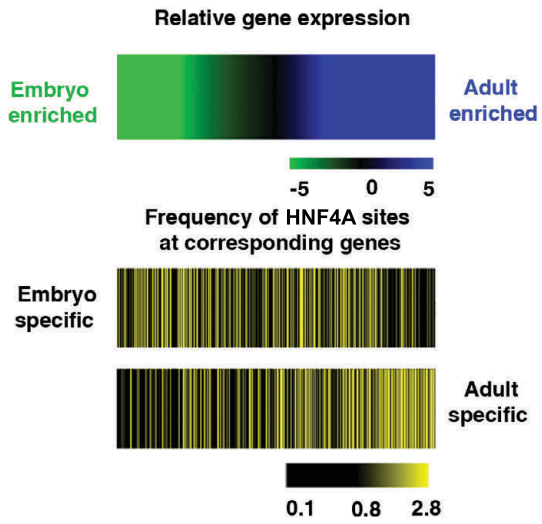

D

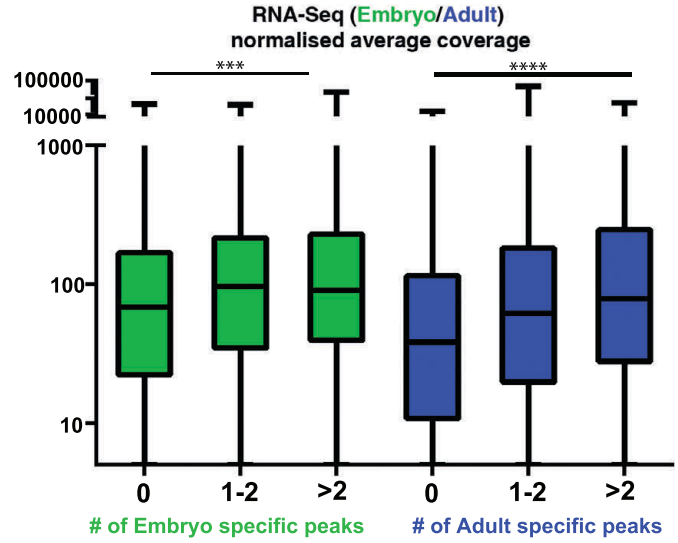

E

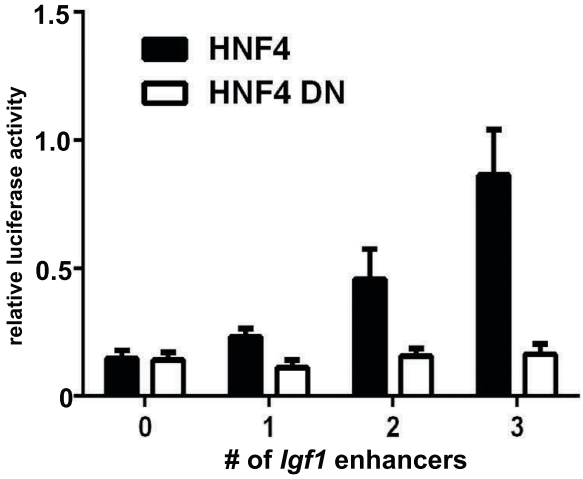

Figure S5

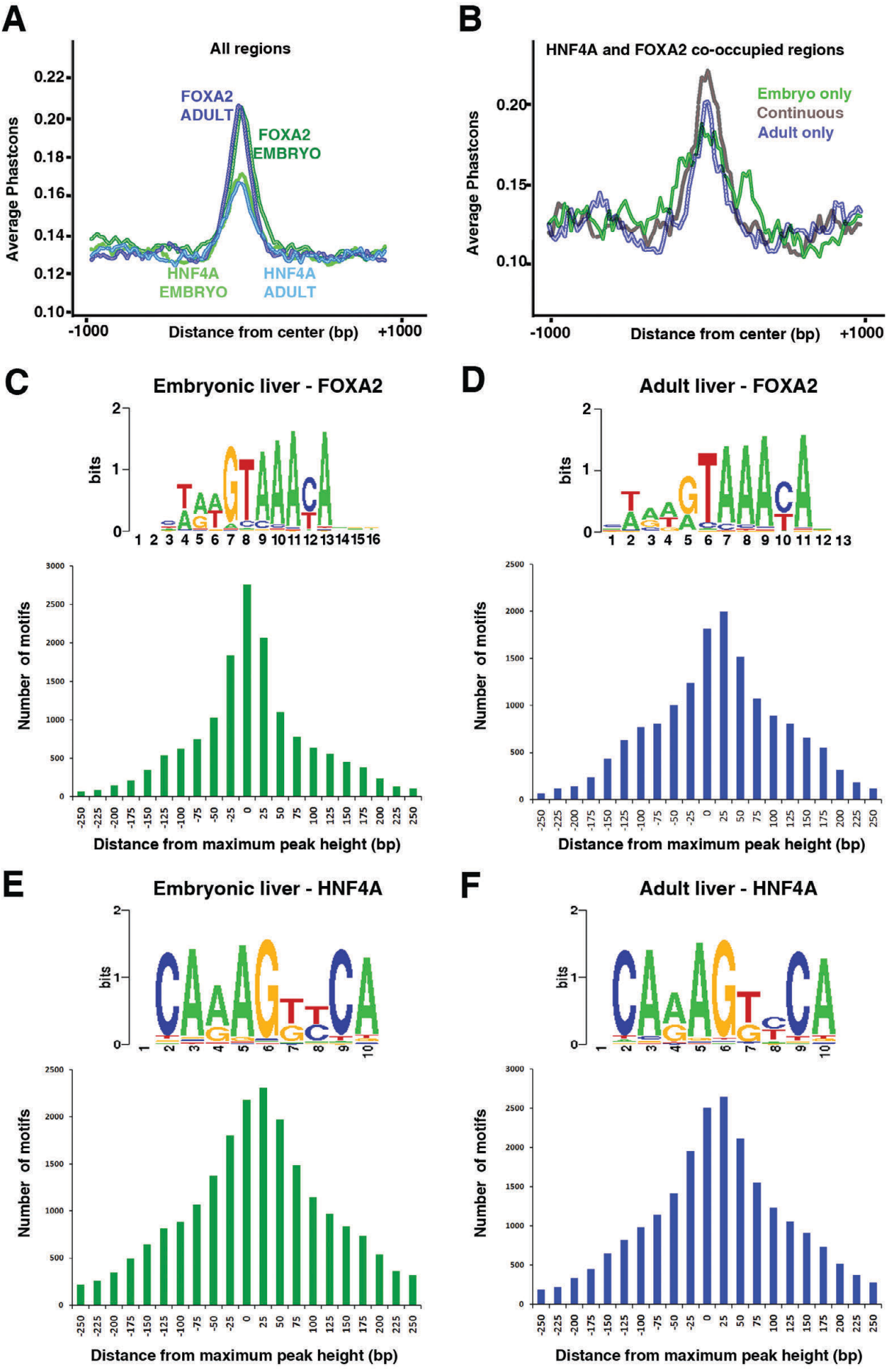
A
All regions
FOXA2 ADULT
FOXA2 EMBRYO
HNF4A EMBRYO
HNF4A ADULT
Average Phastcons
Distance from center (bp)
-1000
+1000
B
HNF4A and FOXA2 co-occupied regions
Embryo only
Continuous
Adult only
Average Phastcons
Distance from center (bp)
C
Embryonic liver - FOXA2
bits
Number of motifs
Distance from maximum peak height (bp)
D
Adult liver - FOXA2
Number of motifs
Distance from maximum peak height (bp)
E
Embryonic liver - HNF4A
bits
Number of motifs
Distance from maximum peak height (bp)
F
Adult liver - HNF4A
bits
Number of motifs
Distance from maximum peak height (bp)

Figure S6

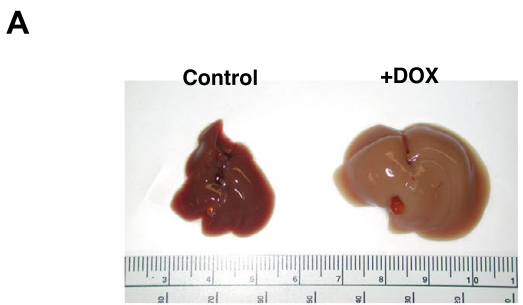
A
Control
+DOX
B
Liver/body ratio (%)
30
25
20
15
10
5
0
Control
+DOX
C
fold increase in expression
400
300
200
100
0
DLK1
H19
IDO2
NNMT
D
Control
+DOX
anti-TEAD2
anti-tubulin
anti-YAP
anti-tubulin

Supplemental Figure Legends

Figure S1. Genomic distribution of HNF4A and FOXA2 binding detected by ChIP-Seq in embryonic liver, see also Figure 1. A) Western blot analysis of embryonic and adult liver protein extract using anti-FOXA2 **B)** Schematic representation of all HNF4A, FOXA2 or co-occupied sites of enrichment in embryonic liver compared to total genome annotation (mm9). Generated using default settings employed by Cis-regulatory Element Annotation System 1.0.2 (Shin *et al*., 2009). Specifically; *promoter* regions are defined as 3000bp upstream of transcriptional start sites as defined by RefSeq, *downstream* regions refer to the 3000bp area immediately downstream regions of transcription termination sites of genes annotated in RefSeq, *3' and 5'UTRs*, *coding exons*, and *introns* are defined by RefSeq. If regions of enrichment do not fall into any of the above categories, they are considered to be *distal intergenic*.

Figure S2. Global comparison and schematic representation of peak types in datasets, see also Figure 2. A) Intersecting four ChIP-Seq datasets gives rise to 15 possible different peak types presented as a venn diagram illustrating the number of each type in our datasets. **B**) Global comparison of HNF4A and FOXA2 ChIP-Seq datasets was carried out using unthresholded bigwig files. The peak max for each enriched region in either embryonic (green), adult (blue) or both (grey) is represented on a scatterplot.

Figure S3. Differentiation-dependent binding sites show distinct patterns of enhancer associated H4ac, see also Figure 3. Heatmap representation of H4ac enrichment (high;black, low;grey) at regions bound by both FOXA2 and HNF4a (▲); only in embryonic liver (green;left), both embryonic and adult liver (grey;middle) or only in adult liver only (blue;right). Enrichment levels (low;white - high;blue) were profiled 1Kb in both directions at a resolution of 10bp from TF peak center, represented by small black triangle. The vertical ordering of sites is random. **B**) Average enrichment profiles of H4ac at differentiation-dependent FOXA2 and HNF4a binding sites (green line;embryo - grey line;continuous - blue line;adult).

Figure S4. Expression analysis of embryonic hepatoblasts and adult hepatocytes, see also Figure 4. RNA-Seq analysis revealed no significant difference in expression levels of HNF4A (**A**) and FOXA2 (**B**) between hepatoblasts purified from E14.5 liver and Adult liver. **A**) HNF4A and FOXA2 DNA binding were detected by ChIP-Seq (lower panels) at the alternative promoter for *HNF4A*. Only low levels of previously characterized 'embryonic' *HNF4A* isoform transcript were detected by RNA-Seq, highlighted in box. **C**) Transcript levels of genes targeted by HNF4A in differentiation-dependent manner either in hepatoblasts (embryo) or adult liver were measured using RNA-Seq. Relative target gene expression levels (log10) were used to rank and bin target genes (10 per unit). Order is conserved between heatmaps. Intensity in bottom two heatmaps (low:black,high:yellow) reflects the average number of differentiation-dependent DNA binding sites within 100kb of genes within that bin divided by the average number of sites per total number of genes in analysis. **D**) Genes were categorized according to the associated number of differentiation-dependent enhancers and global gene expression levels were compared between those not bound specifically at the developmental stage indicated, targeted at 1-2 putative enhancers or bound at more than 2 sites. Significance tested using Kruskal Wallis one way analysis of variance with Dunns post-test correction **** p=<0.001 ***p=<0.005 **E**) *Igf1* enhancers were cloned into luciferase vectors containing a minimal promoter (E1B) and transfected into 293T cells alongside a Renilla containing construct.

Expression vectors for HNF4A and dominant negative (DN-HNF4A) were cotransfected Luciferase assays were conducted 48 hours posttransfection. Data shown is from duplicate experiments are represented as mean +/- SEM.

Figure S5. Conservation of FOXA2 and HNF4A motifs underlying embryonic and adult enhancers, see also Figure 5. A) Phastcons scores were calculated for both total ChIP-Seq datasets (**A**) and differentiation-dependent enhancers (**B**). Graphs were generated using the Conservation Plot Tool within the Galaxy/Cistrome toolbox. FOXA2 (**C**) and HNF4A (**D**) motifs (shown as position weight matrices) derived by *de novo* analysis on embryonic or adult specific peaks using SeqPos within the Galaxy/Cistrome toolbox. Below each motif is a histogram showing the distances of the motif center relative to the location of the maximal enrichment (maximum peak height).

Figure S6. **Induction of YAP-Tg by Doxycycline, see also Figure 6. A, B)** Liver size and body weight ratio is dramatically increased after two weeks of treatment, indicative of functional YAP1 expression. **C**) qRT-PCR analysis was conducted to determine expression levels of target genes. **D**) Nuclear protein was extracted from induced livers and subject to Western Blot analysis using anti-YAP1 and anti-TEAD2.

	Total Reads	Excl. Dup	% Mapped	# Peaks (FDR 0.01)	Filtered Peaks	% Motifs
Embryo FOXA2	2.58E+07	1.3E+07	53.5	10,398	9,338	82.5
Embryo HNF4A	9.46E+07	1.5E+07	30.8	12,033	11,699	83.5
Adult FOXA2	3.3E+07	7.0E+06	33.0	10,964	10,565	77.3
Adult HNF4A	2.40E+07	1.2E+07	48.8	12,824	12,270	91.6
Embryo Input	4.25E+07	1.0E+07	26.9	1,263	N/A	N/A
Adult input	4.92E+07	2.2E+07	45.2	2,515	N/A	N/A

Table S1. ChIP-Seq libraries - mapping and processing details, see also Figure 1.

	Embryo		Adult	
	Read count	**% Total**	**Read count**	**% Total**
Total read count	314,882,346	100	198,186,798	100
Read1-Read2 indentical	74,484	0.02	1,008	0.00
Low complexity	1,830,803	0.58	1,038,065	0.52
Low quality (>1N)	10,272,983	3.26	6,634,987	3.35
Ensembl transcript	128,156,991	43.88	118,760,931	59.92
Ensembl transcript (ambiguous)	10,500,368	3.33	12,631,357	6.37
Novel exon junction	508,780	0.16	467,195	0.24
Novel exon junction (ambiguous)	11,946	0.00	29,216	0.01
Novel exon boundary extension	874,609	0.28	556,932	0.28
Novel exon boundary extension (ambiguous)	26,354	0.01	37,092	0.02
Intron	13,381,115	4.25	7,601,203	3.84
Intron (ambiguous)	334,326	0.11	133,026	0.07
Intergenic	7,726,053	2.45	5,445,035	2.75
Intergenic (ambiguous)	128,248	0.04	76,145	0.04
Repeat element	21,438,097	6.81	1,664,223	0.84
Repeat element (ambiguous)	363,865	0.12	165,864	0.08
Unassigned	109,253,310	34.70	42,944,505	21.67

Table S2. RNA-Seq datasets - mapping and processing details, see also Figure 4.